

See discussions, stats, and author profiles for this publication at: <https://www.researchgate.net/publication/26663033>

# Acoustic Whole Blood Plasmapheresis Chip for Prostate Specific Antigen Microarray Diagnostics

ARTICLE *in* ANALYTICAL CHEMISTRY · JULY 2009

Impact Factor: 5.64 · DOI: 10.1021/ac9013572 · Source: PubMed

---

CITATIONS

75

---

READS

48

9 AUTHORS, INCLUDING:



**Andreas Lenshof**

Lund University

24 PUBLICATIONS 1,385 CITATIONS

SEE PROFILE



**Hans Lilja**

Memorial Sloan-Kettering Cancer Center

460 PUBLICATIONS 21,342 CITATIONS

SEE PROFILE

# Acoustic Whole Blood Plasmapheresis Chip for Prostate Specific Antigen Microarray Diagnostics

Andreas Lenshof,<sup>\*,†</sup> Asilah Ahmad-Tajudin,<sup>†</sup> Kerstin Järås,<sup>†,‡</sup> Ann-Margret Swärd-Nilsson,<sup>§</sup> Lena Åberg,<sup>§</sup> György Marko-Varga,<sup>†</sup> Johan Malm,<sup>‡</sup> Hans Lilja,<sup>‡,||</sup> and Thomas Laurell<sup>\*,†</sup>

Department of Electrical Measurements, Lund University, Box 118, 221 00 Lund, Sweden, Department of Laboratory Medicine, Division of Clinical Chemistry, Lund University, Malmö University Hospital, 205 02 Malmö, Sweden, Blood Center Skane, Lund University Hospital, 221 85 Lund, Sweden, and Departments of Clinical Laboratories, Surgery (Urology), and Medicine (GU-Oncology), Memorial Sloan-Kettering Cancer Center, New York, New York 10021

The generation of high quality plasma from whole blood is of major interest for many biomedical analyses and clinical diagnostic methods. However, it has proven to be a major challenge to make use of microfluidic separation devices to process fluids with high cell content, such as whole blood. Here, we report on an acoustophoresis based separation chip that prepares diagnostic plasma from whole blood linked to a clinical application. This acoustic separator has the capacity to sequentially remove enriched blood cells in multiple steps to yield high quality plasma of low cellular content. The generated plasma fulfills the standard requirements ( $<6.0 \times 10^9$  erythrocytes/L) recommended by the Council of Europe. Further, we successfully linked the plasmapheresis microchip to our previously developed porous silicon sandwich antibody microarray chip for prostate specific antigen (PSA) detection. PSA was detected by good linearity ( $R^2 > 0.99$ ) in the generated plasma via fluorescence readout without any signal amplification at clinically relevant levels (0.19–21.8 ng/mL).

The development of microtechnology and lab-on-a-chip devices has targeted rapid and miniaturized operations for the analysis of blood components and blood plasma. Diverse microtechnology techniques have been developed to enable separation and concentration of the different components in whole blood.<sup>1</sup> Several groups have focused on separating red blood cells from plasma and red cells from white blood cells.<sup>2–6</sup> Extensive efforts have also been spent on the development of chips that integrate plasma generation with subsequent miniaturized diagnostic tests.

A common way of separating plasma from blood using microchannels is to create a mesh or a filter with pores too small for cells to pass through. It can be either a dead end filtration (weirs<sup>7,8</sup> or membranes<sup>8,9</sup>) or cross-flow filtration<sup>10,11</sup> where the plasma exits perpendicular to the main flow channel, a design which is far more advantageous as it is much less likely to clog. Another way of separating plasma from cells is to use plasma skimming<sup>12</sup> where blood cells tend to stick together at low flow rates, thereby creating lower cell concentrations at the channel walls where plasma can be removed. The Zweifach–Fung effect,<sup>13–15</sup> or the bifurcation law, can be used for plasma generation since cells flowing in a main channel with a flow rate higher than that in the smaller side branching channels stick together and generally continue to flow in the main channel while a small clean plasma fraction can be aspirated via side channels.

Acoustic forces generated by ultrasonic standing waves can also be used for plasma separation. The acoustic wave generates a radiation force on the cells moving them into pressure nodes of the standing wave field. There are basically two different approaches to utilize this phenomenon. The first one uses the acoustic wave to move the cells into larger clusters. When the clusters become sufficiently large, they will start to aggregate and sediment, leading to all cells ending up at the bottom of the container. This technique can be designed for batch processing<sup>16</sup> or a continuous flow system where plasma is removed at the top and cell dense medium at the bottom.<sup>17</sup> However, this is a slow process and is not suitable for implementation in microfluidic systems since it is dependent on larger volumes and the

\* Corresponding author. E-mail: andreas.lenshof@elmat.lth.se (A.L.); thomas.laurell@elmat.lth.se (T.L.). Phone: +46 (0)46 2227540. Fax: +46 (0)46 2224527.

<sup>†</sup> Lund University.

<sup>‡</sup> Malmö University Hospital.

<sup>§</sup> Lund University Hospital.

<sup>||</sup> Memorial Sloan-Kettering Cancer Center.

- (1) Toner, M.; Irimia, D. *Annu. Rev. Biomed. Eng.* **2005**, *7*, 77–103.
- (2) Choi, S.; Park, J. K. *Lab Chip* **2007**, *7*, 890–897.
- (3) Petersson, F.; Åberg, L.; Swärd-Nilsson, A. M.; Laurell, T. *Anal. Chem.* **2007**, *79*, 5117–5123.
- (4) Davis, J. A.; Inglis, D. W.; Morton, K. J.; Lawrence, D. A.; Huang, L. R.; Chou, S. Y.; Sturm, J. C.; Austin, R. H. *Proc. Natl. Acad. Sci. U.S.A.* **2006**, *103*, 14779–14784.
- (5) Sethu, P.; Sin, A.; Toner, M. *Lab Chip* **2006**, *6*, 83–89.
- (6) Yamada, M.; Seki, M. *Lab Chip* **2005**, *5*, 1233–1239.

- (7) Wilding, P.; Kricka, L. J.; Cheng, J.; Hvieh, G.; Shoffner, M. A.; Fortina, P. *Anal. Biochem.* **1998**, *257*, 95–100.
- (8) Ji, H. M.; Samper, V.; Chen, Y.; Heng, C. K.; Lim, T. M.; Yobas, L. *Biomed. Microdevices* **2008**, *10*, 251–257.
- (9) Moorthy, J.; Beebe, D. J. *Lab Chip* **2003**, *3*, 62–66.
- (10) Crowley, T. A.; Pizziconi, V. *Lab Chip* **2005**, *5*, 922–929.
- (11) VanDelinder, V.; Groisman, A. *Anal. Chem.* **2006**, *78*, 3765–3771.
- (12) Jaggi, R. D.; Sandoz, R.; Effenhauser, C. S. *Microfluid. Nanofluid.* **2007**, *3*, 47–53.
- (13) Fan, R.; Vermesh, O.; Srivastava, A.; Yen, B. K. H.; Qin, L. D.; Ahmad, H.; Kwong, G. A.; Liu, C. C.; Gould, J.; Hood, L.; Heath, J. R. *Nat. Biotechnol.* **2008**, *26*, 1373–1378.
- (14) Yang, S.; Undar, A.; Zahn, J. D. *Lab Chip* **2006**, *6*, 871–880.
- (15) Shevkoplyas, S. S.; Yoshida, T.; Munn, L. L.; Bitensky, M. W. *Anal. Chem.* **2005**, *77*, 933–937.
- (16) Cousins, C. M.; Holownia, P.; Hawkes, J. J.; Price, C. P.; Keay, P.; Coakley, W. T. *Ultrasonics* **2000**, *38*, 654–656.
- (17) Peterson, S.; Perkins, G.; Baker, C. *IEEE 8 Ann. Eng. Med.* **1986**, 154–156.

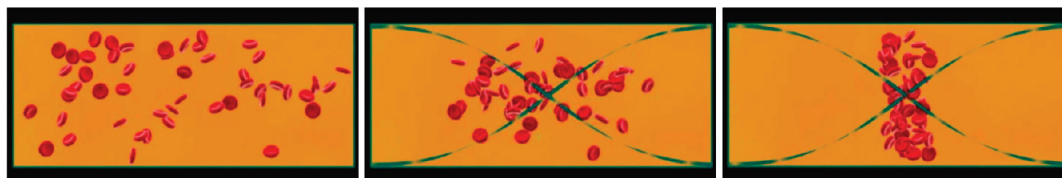


**Figure 1.** Schematic cross section of a microchannel excited by a  $\lambda/2$  wavelength ultrasonic standing wave, whereby the erythrocytes sequentially are focused in the channel center by the primary acoustic radiation force.

sedimentation process will not be very effective in narrow channels where boundary conditions will be predominant.

The other way acoustic standing waves can be used for continuous separation is to use a microfluidic channel that is matched to a half wavelength width.<sup>18–20</sup> When a particle suspension flowing through the channel is exposed to the ultrasonic standing wave (USW), the acoustic forces will move all particles to the pressure node located in the center of the channel,<sup>21</sup> Figure 1. In a microfluidic device, the USW combined with the laminar flow will form a band of concentrated particles in the center of the channel partitioned from the particle-depleted (“clean”) medium distributed toward the periphery. By providing a trifurcated channel outlet, the clean medium will be allowed to exit through the side outlets while particles enriched in the channel center will exit through the central outlet. Petersson et al.<sup>22</sup> demonstrated a separation device where collection of blood shed during surgery was separated into one fraction containing lipids and one fraction with blood cells. In this context, the lipid particles were mixed with the plasma and removed through the side outlets. The drawback of the published acoustic microfluidic separation systems so far has been that they have been limited to sample concentrations of about 5–10% by volume in order to achieve acceptable separation efficiencies. However, the configuration can also be used to generate clean plasma from whole blood if a modified setup is implemented, as described in this paper.

Although many of the reported microfluidic devices that handle blood work well for their intended application, most of them suffer from the fact that they require highly dilute blood samples for the separation to work. Whole blood has a hematocrit of ~38–54%,<sup>23</sup> which will cause many microfluidics systems to clog or get overloaded. Diluting the sample will not, however, give a very representative, or sometimes not even useful, plasma fraction for clinical evaluation. Other chip solutions, which are capable of handling high hematocrit, usually have very poor volume throughput (in the nanoliter to microliter range per minute).

In health care, the most common way of achieving cell free plasma is the use of centrifuges. Although these provide high degrees of cell free plasma, there are several drawbacks. First, the batch processes and size of centrifuges prevent them from being incorporated into a total analysis system in which sample

can be continuously processed through several sequential steps including presample treatment, separation, analysis, and sample readout. Second, the centrifugal spinning induces high shear forces on cells deforming and eventually rupturing them, thus contaminating the plasma with intracellular content. All of these disadvantages can be excluded using on-chip acoustophoretic plasmapheresis, as earlier reported.<sup>24</sup>

An obvious outlook for microchip based clinical grade plasmapheresis is the coupling to an integrated chip for microscaled diagnostic readout. The quest for early cancer diagnosis has promoted the exploration of advanced proteomic technologies, where the search and identification of new cancer biomarkers<sup>25</sup> open up for new improved diagnostics.<sup>26</sup> Besides early diagnostics, biomarkers hold promise in providing information about the disease status at any given point in time, making it possible also to monitor disease progression as well as evaluating therapeutic targets.<sup>27,28</sup>

Along this line, new biochip strategies are being developed for high throughput, parallel protein analysis in biofluids. Detection of low abundant proteins using antibody microarrays in complex specimens, for example, in whole blood, plasma, or serum samples, has successfully been shown by Carlsson et al.<sup>29</sup> and Ingvarsson et al.<sup>30</sup> However, this often requires laborious sample preparation and a reliable microarray platform.<sup>31</sup> Nevertheless, various assay designs,<sup>32</sup> labeling strategies,<sup>31</sup> and signal amplification systems as rolling circle amplification<sup>33–35</sup> or fluorescent nanoparticles,<sup>36</sup> as well as different detection modes<sup>37</sup> have shown great improvements in microarray platforms.

- (18) Nilsson, A.; Petersson, F.; Jonsson, H.; Laurell, T. *Lab Chip* **2004**, *4*, 131–135.
- (19) Harris, N. R.; Hill, M.; Beeby, S.; Shen, Y.; White, N. M.; Hawkes, J. J.; Coakley, W. T. *Sens. Actuators, B: Chemical* **2003**, *95*, 425–434.
- (20) Hawkes, J. J.; Barber, R. W.; Emerson, D. R.; Coakley, W. T. *Lab Chip* **2004**, *4*, 446–452.
- (21) Laurell, T.; Petersson, F.; Nilsson, A. *Chem. Soc. Rev.* **2007**, *36*, 492–506.
- (22) Petersson, F.; Nilsson, A.; Holm, C.; Jonsson, H.; Laurell, T. *The Analyst* **2004**, *129*, 938–943.
- (23) Dailey, J. F. *Blood*; Medical Consulting Group: Arlington, MA, 1998.

- (24) Jonsson, H.; Holm, C.; Nilsson, A.; Petersson, F.; Johnsson, P.; Laurell, T. *The Annals of Thoracic Surgery* **2004**, *78*, 1572–1577.
- (25) Srinivas, P. R.; Srivastava, S.; Hanash, S.; Wright, G. L. *Clin. Chem.* **2001**, *47*, 1901–1911.
- (26) Krista, Y. W.; Rodemich, L.; Nyalwidhe, J. O.; Comunale, M.; Clements, M.; Lance, R. S.; Schellhammer, P. F.; Metha, A. S.; Semmes, J.; Drake, R. R. *J. Proteome Res.* **2009**, DOI: 10.1021/pr8007545.
- (27) Anderson, J. E.; Hansen, L. L.; Mooren, F. C.; Post, M.; Hug, H.; Zuse, A.; Los, M. *Drug Resist. Updates* **2006**, *9*, 198–210.
- (28) Zolg, J. W.; Langen, H. *Mol. Cell. Proteomics* **2004**, *3*, 345–354.
- (29) Carlsson, A.; Wingren, C.; Ingvarsson, J.; Ellmark, P.; Baldertorp, B.; Ferno, M.; Olsson, H.; Borrebaeck, C. A. K. *Eur. J. Cancer* **2008**, *44*, 472–480.
- (30) Ingvarsson, J.; Wingren, C.; Carlsson, A.; Ellmark, P.; Wahren, B.; Engstrom, G.; Harmenberg, U.; Krogh, M.; Peterson, C.; Borrebaeck, C. A. K. *Proteomics* **2008**, *8*, 2211–2219.
- (31) Kusnezow, W.; Banzon, V.; Schroder, C.; Schaal, R.; Hoheisel, J. D.; Ruffer, S.; Luft, P.; Duschl, A.; Syagailo, Y. V. *Proteomics* **2007**, *7*, 1786–1799.
- (32) Ingvarsson, J.; Larsson, A.; Sjöholm, A. G.; Truedsson, L.; Jansson, B.; Borrebaeck, C. A. K.; Wingren, C. *J. Proteome Res.* **2007**, *6*, 3527–3536.
- (33) Jarvius, M.; Paulsson, J.; Weibrecht, I.; Leuchowius, K. J.; Andersson, A. C.; Wahlby, C.; Gullberg, M.; Botling, J.; Sjöblom, T.; Markova, B.; Ostman, A.; Landegren, U.; Soderberg, O. *Mol. Cell. Proteomics* **2007**, *6*, 1500–1509.
- (34) Zhou, H. P.; Bouwman, K.; Schotanus, M.; Verweij, C.; Marrero, J. A.; Dillon, D.; Costa, J.; Lizardi, P.; Haab, B. B. *Genome Biology* **2004**, *5*, R28.
- (35) Schweitzer, B.; Wiltshire, S.; Lambert, J.; O'Malley, S.; Kukanskis, K.; Zhu, Z. R.; Kingsmore, S. F.; Lizardi, P. M.; Ward, D. C. *Proc. Natl. Acad. Sci. U.S.A.* **2000**, *97*, 10113–10119.
- (36) Lilja, H. J. *Clin. Invest.* **1985**, *76*, 1899–1903.

Being the most common male cancer in Western Europe and the United States, prostate cancer is a core area of cancer biomarker research. Prostate specific antigen (PSA) is a well-known and the most widely used cancer biomarker, measured in serum and plasma of patients for the diagnosis of prostate cancer. However, a moderately elevated PSA concentration does not directly indicate prostate cancer since benign prostate hyperplasia cases may exhibit a similar outcome. PSA itself is a serine protease<sup>38–40</sup> which is released into seminal plasma upon ejaculation with a concentration of 1 g/L while its presence in the serum under normal conditions is around 0.6 ng/mL. The quest for more biomarkers for the detection of cancer leads to extensive worldwide efforts. It is anticipated that the diagnosis in the future will involve screening for more biomarkers in a parallel fashion which then requires a substrate specific for protein microarrays.<sup>41</sup>

The potential in the use of macroporous silicon as a microchip substrate in protein microarray applications has previously been described by our group, fulfilling the requirements for a well-performing bioassay in undiluted plasma.<sup>41,42</sup> Porous silicon provides a surface that exhibits a small spot area due to the hydrophobic nature of the micro/nanomorphology of the chip surface, good spot reproducibility, homogeneous spot profiles, and low intrinsic fluorescence background, as well as providing an improved limit of detection when compared to other commercially available substrates.<sup>43</sup> It was also demonstrated that porous silicon is compatible with a dual readout mode which simultaneously provides both affinity (fluorescence) and mass identity (matrix-assisted laser desorption ionization time-of-flight mass spectrometry, MALDI-TOF MS) information of the captured protein.<sup>44</sup>

This paper presents an ultrasonic standing wave (USW) plasmapheresis microchip, which is capable of processing whole blood and producing plasma fractions for a subsequent immunoassay. The USW separator has increased the separator channel length as compared to our previously reported devices, with multiple outlets along the bottom of the separation channel, where concentrated cell fractions could be diverted from the main flow without affecting the influence of the cell focusing radiation force, until there is basically only cell free plasma left in the channel. Our current results show that 12.5% clean plasma by volume could be extracted from whole blood. The obtained plasma contained less than  $6.0 \times 10^9$  erythrocytes/L which is in line with the quality specifications for blood transfusion stated by the Council of Europe.<sup>45</sup>

In addition, this paper describes a clinical application of the developed plasmapheresis chip when linked to our previously developed porous silicon sandwich antibody microarray chip for

PSA detection.<sup>42</sup> By combining USW microfluidics and protein microarray technology, an all microchip based PSA detection from whole blood is obtained in a novel lab-on-a-chip configuration.

## MATERIALS AND METHODS

**Plasmapheresis Chip Fabrication.** The plasmapheresis separator was fabricated in silicon through double sided photolithography and chemical anisotropic wet-etching using KOH. The separation channel was designed to have a resonance around 2 MHz, and thus, the channel width was about 350  $\mu\text{m}$ . The channel was sealed with a glass lid using anodic bonding. Silicon tubing was glued to the outlets at the backside to act as docking ports to standard 1/16 in Teflon tubing. More detailed information regarding the fabrication process can be found in Nilsson et al.<sup>18</sup> The 2 MHz piezoceramic transducer (PZ26, Ferroperm Piezoceramics, Kvistgard, Denmark) was coupled to the chip together via a hydrogel (Aquasonic Clear Ultrasound Gel, Parker Laboratories Inc., Fairfield, NJ) that assured a good acoustic coupling.

**Experimental Setup.** The piezoceramic transducer was actuated using an Agilent 33250A waveform generator and an Amplifier Research 75A250 amplifier. The input power to the transducer was monitored using a Bird model 5000-EX digital power meter. The blood was aspirated through the separator using syringe pumps (WPI SP210iwz, World Precision Instruments, Sarasota, FL) and 5 mL Hamilton glass syringes (1005 TLL, Hamilton Bonaduz AG, Bonaduz, Switzerland). The separation was visually monitored using a Nikon SMZ-2T microscope.

**Sample Collection.** Twelve port injectors (25.EPC12W, VICI, Valco Instruments, Houston, TX) were used to acquire samples from the outlets. Teflon tubing (0.5 mm i.d.), inserted in the silicone tubing, connected the chip and the injectors. Each injector collected samples from two outlets in 50  $\mu\text{L}$  Teflon tubing (0.5 mm i.d.) loops.

**Blood Samples.** Citrate treated blood samples were obtained from anonymous healthy donors. The different hematocrit levels were achieved by diluting the whole blood with centrifuged plasma from the same sample. The hematocrit levels were controlled using a centrifuge (Haematocrit 210, Hettich, Tuttlingen, Germany). A Coulter Counter (Multisizer 3, Beckman Coulter Inc., Fullerton, CA) was used to determine the separation efficiency, the percentage of cells removed from each outlet, and the quality of the generated plasma. The particle sizes counted were in the range of 4–8  $\mu\text{m}$ . The diameter of an erythrocyte is about 7  $\mu\text{m}$ , and leukocytes are generally larger or the same size<sup>23</sup> which means that they will most certainly be separated even though not counted. The separation efficiency was calculated as

$$\text{Sep. eff.} = \frac{N_A Q_A + N_B Q_B + N_C Q_C + N_D Q_D}{N_A Q_A + N_B Q_B + N_C Q_C + N_D Q_D + N_E Q_E}$$

where  $N_x$  is the amount of particles in 10  $\mu\text{L}$  of sample from outlet  $x$  as measured by the Coulter Counter and  $Q_x$  is the flow rate in outlet  $x$ , as set by the syringe pump.

**Proteins and Reagents.** Prostate specific antigen (PSA) from human semen was obtained from Sigma. Monoclonal antibodies 2E9 and H117 were produced and characterized as previously described.<sup>46,47</sup> 2E9 was labeled with fluorescein isothiocyanate (FITC) isomer I-Celite (Sigma St. Louis, MO, USA) and separated on a PD10 column (Amersham, Uppsala, Sweden).

- (37) Jaras, K.; Tajudin, A. A.; Ressine, A.; Soukka, T.; Marko-Varga, G.; Bjartell, A.; Malm, J.; Laurell, T.; Lilja, H. *J. Proteome Res.* **2008**, *7*, 1308–1314.  
(38) Lilja, H.; Ulmert, D.; Vickers, A. J. *Nat. Rev. Cancer* **2008**, *8*, 268–278.  
(39) Lilja, H.; Abrahamsson, P. A.; Lundwall, A. *J. Biol. Chem.* **1989**, *264*, 1894–1900.  
(40) Lilja, H.; Lundwall, A. *Proc. Natl. Acad. Sci. U.S.A.* **1992**, *89*, 4559–4563.  
(41) Ressine, A.; Ekstrom, S.; Marko-Varga, G.; Laurell, T. *Anal. Chem.* **2003**, *75*, 6968–6974.  
(42) Jaras, K.; Ressine, A.; Nilsson, E.; Malm, J.; Marko-Varga, G.; Lilja, H.; Laurell, T. *Anal. Chem.* **2007**, *79*, 5817–5825.  
(43) Steinhauer, C.; Ressine, A.; Marko-Varga, G.; Laurell, T.; Borrebaeck, C. A. K.; Wingren, C. *Anal. Biochem.* **2005**, *341*, 204–213.  
(44) Finnskog, D.; Ressine, A.; Laurell, T.; Marko-Varga, G. *J. Proteome Res.* **2004**, *3*, 988–994.  
(45) *Guide to the preparation, use and quality assurance of blood components*, 13th ed.; Council of Europe Publishing: Strasbourg, 2007.



**Human Female Whole Blood Spiked with PSA.** Human female blood samples were obtained from healthy donors as described above. The individual blood samples were spiked with PSA before plasmapheresis. Female whole blood was used to ensure that there was no detectable amount of PSA present in the original sample.

**Porous Silicon Protein Chip.** Fabrication of the porous silicon was carried out by anodic dissolution of a p-type monocrystalline silicon wafer (Addison Engineering, Inc. San Jose, CA; resistivity 1.0–10.0  $\Omega$  cm). In this process, the silicon wafer was placed in between two electrochemical cells filled with electrolyte solution containing a mixture of 1:10 by volume a of 40% hydrofluoric acid and 99.8% dimethyl formamide. The electrolyte provides contact to the wafer on both sides. During anodization, the backside of the wafer was illuminated using a 100 W halogen lamp (Osram, Germany), which was placed 10 cm from the window of the chamber. A constant current of 91 mA was passed through the system for 70 min, and as this occurs, pore formation was initiated resulting in the formation of a porous silicon layer at the anodic side of the wafer. The porosified silicon wafer was further diced into small pieces of 6  $\times$  6 mm, forming the porous silicon chips. A more detailed description on the fabrication setup is described elsewhere.<sup>48</sup>

**Microarraying Using a Piezoelectric Flow-through Microdispenser.** An in-house developed piezoelectric microdispenser and a software controlled arraying station were used to form microarrays with 600 spots/array of monoclonal mouse antiPSA capture antibody H117. The microdispenser,<sup>49–51</sup> which is actuated by a piezoceramic element, is able to generate single 100 pL droplets of antibody to form an array with a 150  $\mu$ m distance between each spots. H117 was allowed to bind to the surface via physical adsorption.

**Sandwich Antibody Microarray.** The porous silicon sandwich antibody microarray protocol<sup>42</sup> was carried out for the detection of PSA in microchip plasmapheresis generated plasma samples. The capture antibody H117 in PBS (0.5 mg/mL) was arrayed onto the porous silicon chips followed by a 3 time washing step in PBS–Tween (0.05% Tween 20 in PBS) to remove loosely bound antibodies. Arrayed chips were then blocked with 5% nonfat dry milk in PBS–Tween for 30 min in order to prevent unspecific binding during the next incubation step. The washing step was repeated before exposing the chips to incubation with a 24  $\mu$ L sample solution for 70 min. After the incubation, the chips were washed again 3 times. The next step was to incubate the chips with 24  $\mu$ L of FITC-labeled 2E9 monoclonal mouse anti-PSA-antibody. After a 1 h incubation, the chips were washed 3 times in 5 ml of PBS–Tween, quickly dipped in distilled water, and dried with pressurized air before confocal microscope detection.

**Fluorescence Readout and Analysis.** Fluorescence detection was performed using a confocal microscope setup (Olympus), an oil immersion 20 $\times$  objective, an ion laser (Melles Griot Laser Group) with an excitation wavelength of 488 nm, and a Fluoview scanner unit (Fluoview, Olympus). Image analysis was carried out using Fluoview 300 software. The total intensity of each spot was quantified using Fluoview 300 and the circle method. Background total intensity was measured using a similar method and was then subtracted from the total intensity of each spot. Nine spots and their backgrounds were measured for each image analysis, thus generating the mean spot intensities presented in the figures.

**DELFI Analysis.** DELFIA Prostat PSA free/total assay is a quantitative time-resolved fluoroimmunoassay developed by Perkin-Elmer (Perkin-Elmer, Turku, Finland) for simultaneous detection of total PSA and free PSA (uncomplexed PSA) in serum. It is a solid phase immunoassay based on a direct sandwich technique utilizing three monoclonal antibodies. The capture antitotal PSA antibody is used to bind both free and complexed PSA to the solid phase. Europium labeled antibodies are directed against the free PSA whereas samarium labeled antibodies are directed against both free and complexed PSA (total PSA). The fluorescence from europium and samarium are detected using time-resolved fluorescence and are proportional to the concentrations of free and total PSA in the sample.<sup>52</sup> In this study, DELFIA was used as a reference assay for the chip based total PSA assay.

## RESULTS AND DISCUSSION

**USW Plasmapheresis.** To separate high particle concentrations based on ultrasonic standing waves, we designed a new acoustophoresis chip design. The goal was to address the limitations of our previously presented microfabricated silicon acoustic separator chips,<sup>18,22</sup> which were not able to process sufficiently high particle concentrations, partly due to the very high acoustic forces required to concentrate particles into a band sufficiently narrow to enable separation. This in turn resulted in high driving voltages to the piezoceramic transducer and a dramatic temperature increase because of power losses in the transducer. The time a particle or cell spends in the acoustic field is of major importance. In a short separation channel, much higher acoustic forces are needed to accomplish the same particle movement as in a much longer channel where a moderate acoustic force affects the particle during a longer time period. Higher concentrations with more particles also require more time to focus the particles into pressure nodes. This can be accomplished by lowering the flow rate and/or prolonging the channel, of which the latter has been the target of this paper.

The new separator is a modification of the previously reported designs, in which the relatively short (15–30 mm) separation channel ended in a trifurcation where concentrated blood cells exit through the central outlet and clean plasma exits through the side branches. The new separator was modified in two steps. First, the separation channel was elongated in a meander type of fashion, which enables the blood cells to be affected by the acoustic standing wave for a longer time period. An acoustic force of higher magnitude is thus not necessary, as the radiation force instead acts for a longer duration, forcing the cells gently into a

(46) Lilja, H.; Christensson, A.; Dahlen, U.; Matikainen, M. T.; Nilsson, O.; Pettersson, K.; Lovgren, T. *Clin. Chem.* **1991**, *37*, 1618–1625.

(47) Pettersson, K.; Piironen, T.; Seppälä, M.; Liukkonen, L.; Christensson, A.; Matikainen, M. T.; Suonpää, M.; Lövgren, T.; Lilja, H. *Clin. Chem.* **1995**, *41*, 1480–1488.

(48) Drott, J.; Lindstrom, K.; Rosengren, L.; Laurell, T. J. *Micromech. Microeng.* **1997**, *7*, 14–23.

(49) Laurell, T.; Wallman, L.; Nilsson, J. J. *Micromech. Microeng.* **1999**, *9*, 369–376.

(50) Miliotis, T.; Kjellstrom, S.; Nilsson, J.; Laurell, T.; Edholm, L. E.; Marko-Varga, G. *J. Mass Spectrom.* **2000**, *35*, 369–377.

(51) Onnerfjord, P.; Nilsson, J.; Wallman, L.; Laurell, T.; Marko-Varga, G. *Anal. Chem.* **1998**, *70*, 4755–4760.

(52) Mitrinen, K.; Pettersson, K.; Piironen, T.; Bjork, T.; Lilja, H.; Lovgren, T. *Clin. Chem.* **1995**, *41*, 1115–1120.

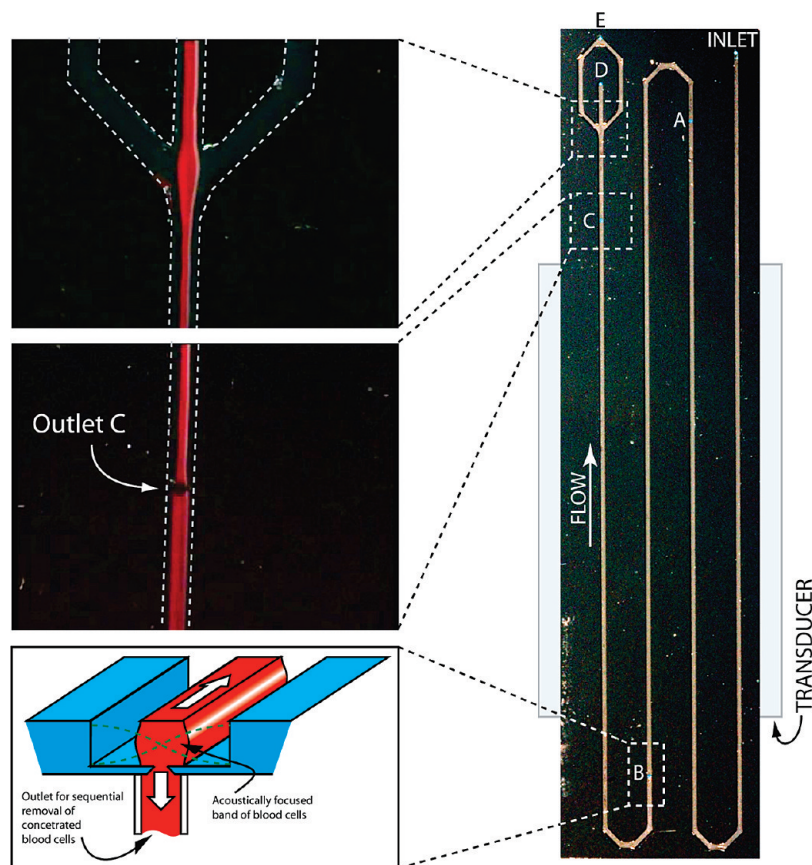


**Figure 2.** Principle of plasmapheresis. Acoustic standing waves gather blood cells in the pressure node located in the middle of the separation channel. Enriched blood cell fractions are removed through outlets A–C, thus decreasing the hematocrit gradually in the channel. The remaining focused blood cells exit through outlet D while the clean plasma fraction is withdrawn from exit E. The transducer placed underneath the chip generates an ultrasonic standing wave between the channel walls, perpendicular to the flow. Dotted lines have been added to the microscope images (upper and middle left) to outline the channel boundaries.

focused band. Second, several extra outlets were added along the separation channel, in contrast to previous designs which had no outlets along the separation channel at all. These outlets, placed in the middle of the separation channel, allow blood cells already focused to be removed without removing a large part of the blood plasma. This procedure decreases the concentration of blood cells in the separation channel in several consecutive steps by gradually lowering the concentration in the center of the channel. At the end of the separation channel all remaining cells are packed in a sufficiently narrow band prior to reaching the flow splitter, which enables a high separation efficiency; see Figure 2. Our earlier publication on acoustic particle focusing revealed that the focusing of the cells in the flow channel occurs throughout the full height of the chip,<sup>53</sup> which explains why it is a justified strategy to remove already acoustically focused cells from the center region of the microchannel as outlined in positions A, B, and C in Figure 2. The design also allow cells to be continuously exposed to the acoustic standing waves during the sequential removal steps since the outlet is placed perpendicular to the standing waves and no extra diversion of flows with flow splitters is needed.

Four different designs with different separation channel lengths were investigated. All designs have one inlet and five outlets. The basic design was a channel, approximately 56 mm long, with the channel outlets symmetrically placed along the channel. The other

designs denoted 2M, 3M, and 4M after the number of meanders on the chip had separation channel lengths of 108, 166, and 224 mm, respectively (Figure 3). All separators were actuated with the same transducer (22 × 32 mm, pz26, Ferroperm Piezoceramics) at approximately 2.05 MHz, except 1M which had a smaller transducer (11 × 11 mm, pz26, Ferroperm Piezoceramics) since the tubing on the backside prevented the use of the larger one. The net input power into the device was, however, the same in all cases, ~300 mW.

The total flow rate of the plasmapheresis chips was set to 80  $\mu\text{L}/\text{min}$  with a flow distribution of the outlets, as seen in Table 1. The higher flow rates of the first outlets were chosen as it is important to quickly remove the bulk of the focused blood cells in the separation channel in order to lower the concentration so that all remaining cells can be focused before the flow split.

The first tests were made on design 1M, with a suspension comprising 5  $\mu\text{m}$  polyamide particles designed for mimicking blood. 1M consisted of a straight channel with three channel outlets where particles could be removed sequentially before the trifurcation; see Figure 3. When tested with higher concentration levels (>20%), a plug of stacked particles would build up around outlets A, B, or C and occlude the channel. It was concluded that the outlets were too narrow and the high concentrations of beads were effectively blocking each other from exiting the outlet. Instead of being approximately 1/3 of the channel width, the output holes were widened to ~2/3 of the channel width. This of

(53) Evander, M.; Lenshof, A.; Laurell, T.; Nilsson, J. *Anal. Chem.* **2008**, *80*, 5178–5185.

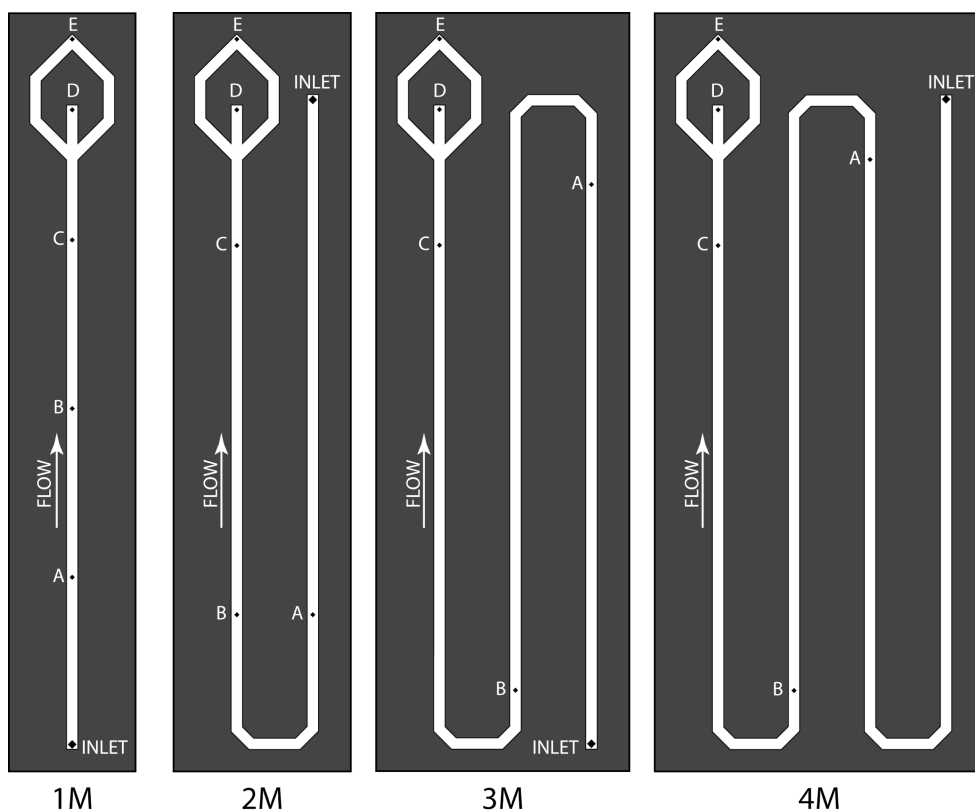


**Figure 3.** Schematic of the separator designs. They are denoted 1M, 2M, 3M, and 4M after the number of meanders present on the chip. The blood enters through the inlet and fractions are removed through outlets A, B, C, D, and E. Outlets A–D will contain blood of varying concentration while the clean plasma fraction is taken out from outlet E.

**Table 1. Flow Distribution between the Different Outlets Used in the Plasmapheresis<sup>a</sup>**

outlet	A	B	C	D	E	inlet
flow rate [ $\mu\text{L}/\text{min}$ ]	20	20	15	15	10	80

<sup>a</sup> The total flow rate in the chip, i.e., the inlet flow of 80  $\mu\text{L}/\text{min}$ , is the sum of the combined flow rates of the individual pump settings of the outlets.

course increased the risk of losing plasma along the separation when blood was used, but as the geometry of the outputs are oriented in a diamond shape in relation to the flow channel, most of the fluid extracted will still be from the central 1/3. Another interesting feature that was noticed during separation is that the outlets along the separation channel enhance the focusing effect as particle rich fractions are removed. This is noted, because the neighboring particles to the ones removed are translated closer to the center of the separation channel with their medium in order to fill the void of the fluid removed by the outlets and, thus, actually further assisted the focusing of the remaining particles. It should be noted, however, that rigid particles are less flexible than blood cells. Blood with hematocrit of 20% surely behaves differently than a particle suspension of the same concentration, and it is possible that the original sizes of the outlets might have worked out well for blood samples. Blood has been reported to maintain flow as hematocrit reaches as high as 98%.<sup>54</sup> However, the increased size of the outlet holes is still probably beneficial, as it applies less shear forces to the cells.

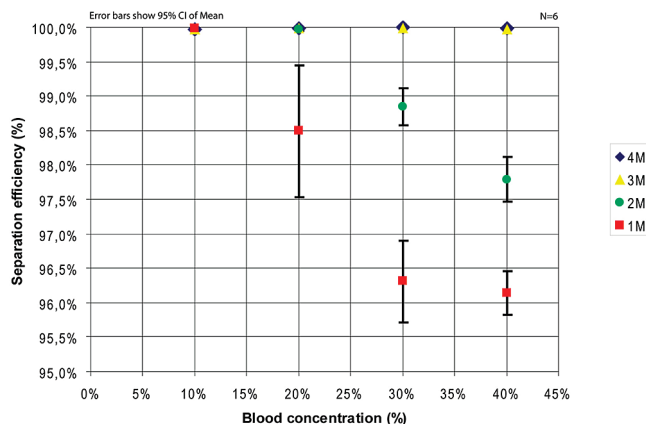


**Figure 4.** Separation efficiency of the four different separators. It is obvious that the separation efficiency decreases with increased hematocrit for the shorter separation channel designs, 1M and 2M, which are characterized by shorter exposure of the cells to the acoustic force field.

With the fluidic extraction under control, the different designs were tested with blood at the flow rates showed in Table 1. At low hematocrits,  $\sim 10\%$ , all chips performed well but as the concentration was increased, the 1M and 2M chips started to lose blood cells in the flow splitter to outlet E. The separation channels were not sufficiently long, and thus, the duration of the exposure of the cells in the acoustic focusing field was not long enough to accomplish a complete separation. The tendency of poor separation efficiencies became progressively worse as the concentration increased further (Figure 4). As the hematocrit approached whole blood, i.e.,  $\sim 40\%$ , the 3M and 4M chips proved to be the only designs capable of

(54) Fung, Y. C. *Biomechanics - Mechanical Properties of Living Tissues*, 2nd ed.; Springer: New York, 1993.



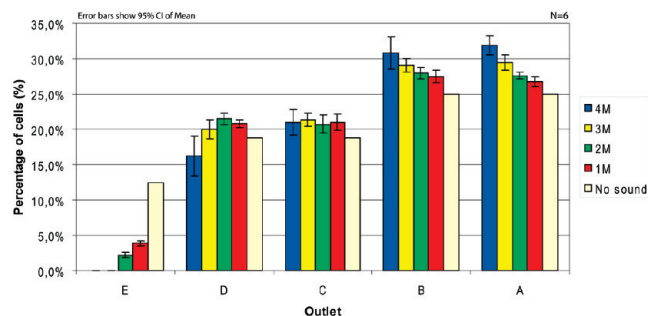


**Figure 5.** Percentage of blood cell separation by each outlet for whole blood (Hct 40%). Most cells are removed in outlets A and B, which is expected since these also have the highest flow rate. The high percentage of removed cells in A and B for 4M can be explained by the length of the separation channel between the outlets which gives the cells extended time for focusing in the ultrasonic standing wave field.

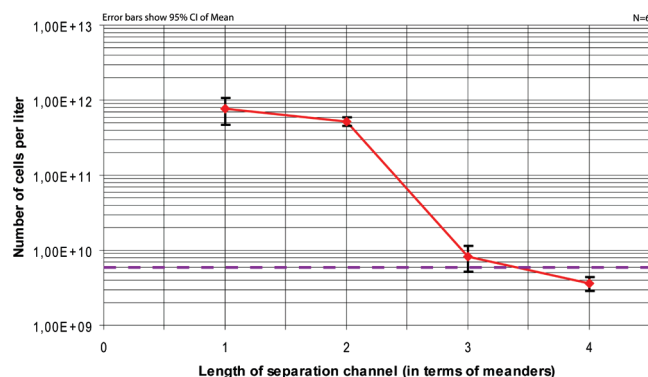


**Figure 6.** Amount of cells per liter of clean plasma separated from whole blood (Hct 40%). The purple dotted line shows the upper limit of numbers of erythrocytes per liter of plasma for a transfusion set by the Council of Europe. That limit, which is set to  $6 \times 10^9$  erythrocytes/L, was surpassed by the 4M plasma separator which generated plasma with cell counts of  $3.65 \times 10^9$ .

handling such high concentrations. It should, however, be noted that the separation efficiencies are only relative to the total amount of particles processed per minute, which means that there can still be a relatively high number of cells present in the plasma fraction even though the separation efficiencies are close to 100%.

The percentages of cells removed by each outlet at an inlet concentration of 40% were measured by a Coulter Counter and are shown in Figure 5. The graph demonstrates that most of the cells exit the chip via outlets A and B which can be expected as they have the largest flow rate. It should also be noted that the longer the cells are exposed to the field, the larger fraction of the cells can be removed. This can easily be seen by the trend of the height of the stacks for outlets A and B. Figure 5 also shows that if the cell removal is not effective due to poor particle focusing in the beginning of the separation, it will be very difficult to make up for it in the end.

As mentioned earlier, the separation efficiency is a relative measure which is highly dependent on the total amount of particles separated. Although Figure 4 showed 100% separation for design 3M and 4M, they did not show the same result when the absolute number of cells in the plasma fractions were measured. Figure 6 shows the total cell count in the plasma fractions, and the dotted purple line in the graph represents the threshold number of erythrocytes ( $6.0 \times 10^9$ /L) which the Council

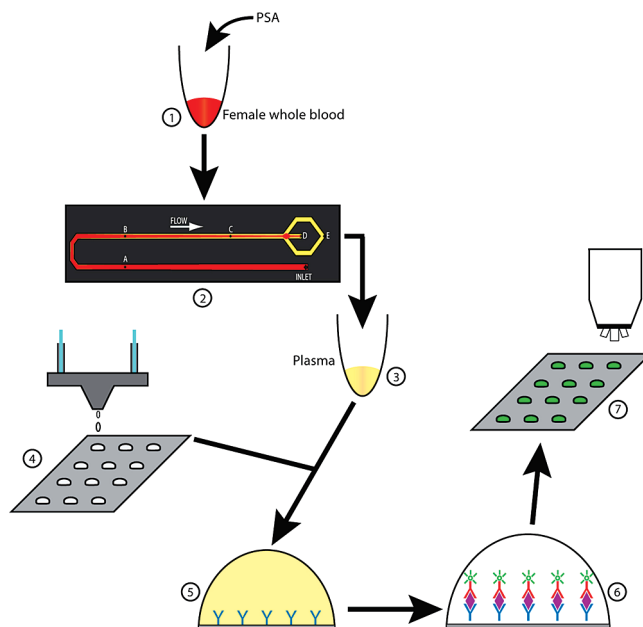


**Figure 7.** Schematic of the all chip based whole blood plasmapheresis and PSA diagnostics: (1) spiking of PSA in female whole blood, (2) ultrasonic standing wave driven microchip plasmapheresis, (3) plasma collected via injector sample loops, (4) microarraying of PSA antibody, (5) microchip incubation in obtained plasma, (6) sandwich assay, and (7) fluorescence readout.

**Table 2. PSA Concentrations, As Measured by DELFIA, Mean Spot Intensities from the Sandwich Antibody Microarray, and the Corresponding Standard Deviations and Coefficients of Variation**

concentration, ng/mL	mean spot intensity, [AU]	standard deviation, [AU] ( <i>n</i> = 9)	CV, % ( <i>n</i> = 9)
0.19	159 880	40 398	25.3
2.57	613 335	108 150	17.6
3.52	724 538	155 725	21.5
5.35	937 604	130 383	13.9
21.8	4 191 924	412 651	9.8

of Europe recommends for plasma transfusion.<sup>45</sup> The number of cells per liter of plasma by the 3M design is  $8.28 \times 10^9$ , which exceeds the recommended limit. The 4M design however had a cell count of  $3.65 \times 10^9$  per liter which is well below the limit and thus provides plasma of approved quality. It is, however, unlikely that the separation device could be used for transfusion medicine since the throughput and recovery rate in its current format is not sufficiently high for supporting a full clinical transfusion application. The results, however, clearly show that the reported plasmapheresis chip can serve as a platform for online automated chip based analysis in a clinical setting.

**PSA Microarray Detection of Whole Blood Processed by Plasmapheresis.** In an oncoming effort to develop a fully integrated diagnostic microfluidic platform, we have now developed a hybrid system combining the plasmapheresis module and our previously reported PSA antibody microarray platform. In order to validate that the plasma holds sufficient quality, we analyzed it on our PSA antibody microarray. The system (shown schematically in Figure 7) enables detection of low abundant PSA in whole blood samples. We investigated female whole blood samples spiked with PSA concentrations in the range of 0.19–21.8



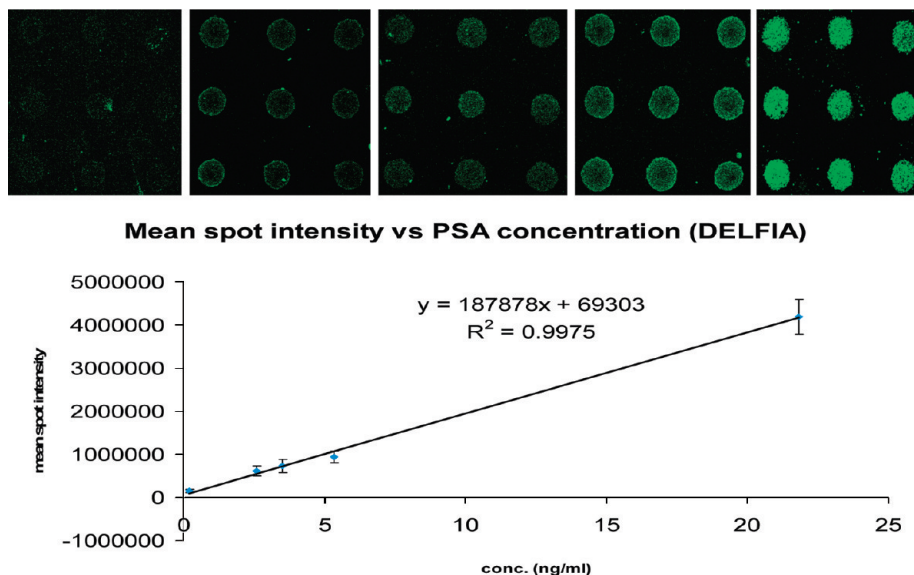


**Figure 8.** Microarray results of the titration series of blood plasma derived from PSA spiked female whole blood. The images shown were obtained from the porous silicon sandwich antibody microarray. Mean spot intensities and standard deviations (error bars) were calculated from the spots in the inset images detected via a 20 $\times$  lens. The PSA concentrations on the x-axis were obtained by the reference DELFIA assay of the same plasmapheresis treated samples.

ng/mL. PSA-spiked whole blood samples were applied to the plasmapheresis microchip, generating pure plasma fractions for the subsequent PSA microarray assay.

We have shown earlier that our porous silicon sandwich antibody microarray platform is capable of analyzing serum samples for PSA.<sup>37,42</sup> In this sandwich antibody array, the capture antibody H117 is physically absorbed onto the porous silicon surface. As the plasma sample is applied, the PSA is concentrated onto the spots by H117. The captured PSA is subsequently detected with a fluorescently labeled antibody, in this case, FITC-labeled 2E9. The dynamic range, limit of detection, linearity, and assay reproducibility of our sandwich antibody microarray platform have been addressed and described in our earlier work. No nonspecific binding of serum proteins have been found (data not shown), when analyzing crude female serum samples in the assay. A commercially available 96 well based immunoassay (Prostatus PSA Free/Total DELFIA) was used as a reference to determine the PSA concentration.

Our current results, based on duplicate arrays for each concentration of PSA in the titration series, generated high intensity spots (Table 2). The mean spot intensities and coefficient of variation (CV) of Table 2 were calculated from the spots of the insert images of Figure 8. CVs of around 18% correlate well with earlier results of the sandwich assay.<sup>42</sup> The graph in Figure 8, showing the mean spot intensity versus PSA concentration, as determined by DELFIA, corresponded to a coefficient of determination of  $R^2 > 0.99$ . The error bars show the standard deviations calculated from the spot intensities. Based on DELFIA, the lowest concentration of PSA detected in this study was 0.19 ng/mL. The sensitivity of the sandwich assay for PSA presented here clearly covered diagnostic cut points of 0.6–4 ng/mL that are frequently being assessed in reference to their ability to identify men with elevated risk of malignant or benign prostate disease.

The developed system, which combines the whole blood acoustic separator (plasmapheresis) microchip and the porous silicon sandwich antibody microarray chip, proved the ability to detect low abundant PSA from whole blood samples. The extended application of this work would be a miniaturized lab-on-a-chip approach, integrating both plasmapheresis and the prostate cancer biomarker assay using minute amounts of patient whole blood.

## CONCLUSION

High hematocrit levels are generally difficult to process by means of acoustophoresis; however, the presented sequential blood cell removal procedure gradually reduced the hematocrit level via a multiple outlet configuration, providing cell free plasma. The quality of the plasma fulfilled the standard defined by the Council of Europe for plasma transfusion. The new plasmapheresis chip was linked to microchip based PSA assaying based on in-house developed nanoporous silicon antibody arrays. Obtained PSA microarray data showed good linearity to reference measurements by a well-documented commercial PSA assay. Forth coming developments will focus on integrating the microarray platform with the plasmapheresis system enabling the development of chip integrated point of care diagnostics.

## ACKNOWLEDGMENT

The Swedish Research Council Project nos. 2006-7600 and 20095 (Medicine), Swedish Cancer Society Project no. 08-0345, Foundation for Strategic Research, Vinnova, Crafoordstiftelsen, Carl Trygger Foundation, Royal Physiographic Society in Lund, and Knut & Alice Wallenberg Foundation are greatly acknowledged for their financial support.

Received for review January 25, 2009. Accepted June 25, 2009.

AC9013572